Fatty acid-dependent globotriaosyl ceramide receptor function in detergent resistant model membranes

Radhia Mahfoud,* Adam Manis,*,§ and Clifford A. Lingwood[1],*,†,**

Division of Molecular Structure and Function* and Department of Pediatric Laboratory Medicine,† Research Institute, The Hospital for Sick Children, Toronto, Ontario, Canada; Department of Laboratory Medicine and Pathology§ and Department of Biochemistry,** University of Toronto, Toronto, Canada

Abstract   Glycosphingolipid (GSL) fatty acid strictly regulates verotoxin 1 (VT1) and the HIV adhesin, gp120 binding to globotriaosyl ceramide within Gb_3/cholesterol detergent resistant membrane (DRM) vesicle constructs and in Gb_3 water-air interface monolayers in a similar manner. VT2 bound Gb_3/cholesterol vesicles irrespective of fatty acid composition, but VT1 bound neither C18 nor $C20Gb_3$ vesicles. $C18/C20Gb_3$ were dominant negative in mixed Gb_3 fatty acid isoform vesicles, but including $C24:1Gb_3$ gave maximal binding. VT1 bound $C18Gb_3$ vesicles after cholesterol removal, but $C20Gb_3$ vesicles required sphingomyelin in addition for binding. HIV-1gp120 also bound C16, C22, and C24, but neither C18 nor $C20Gb_3$ vesicles. C18 and $C20Gb_3$ were, in mixtures without $C24:1Gb_3$, dominant negative for gp120 vesicle binding. Gp120/VT1bound C18 and $C24:1Gb_3$ mixtures, although neither isoform bound alone. Monolayer surface pressure measurement showed VT1, but not VT2, bound Gb_3 at cellular DRM surface pressures, and confirmed loss of VT1 and gp120 (but not VT2) specific $C18Gb_3$ binding.▮▮ We conclude fatty-acid mediated fluidity within simple model GSL/cholesterol DRM can selectively regulate GSL carbohydrate-ligand binding.—Mahfoud, R., A. Manis, and C. A. Lingwood. **Fatty acid-dependent globotriaosyl ceramide receptor function in detergent resistant model membranes.** *J. Lipid Res.* 2009. **50:** 1744–1755.

Supplementary key words   cholesterol • DRM • HIVgp120 • Langmuir trough • lipid raft • sucrose gradient • verotoxin 1 • verotoxin 2

The glycosphingolipid (GSL) globotriaosyl ceramide, Gb_3, is the only cell receptor for the *E. coli*–derived verotoxins (VT or Shiga toxins) (1, 2). Plasma membrane Gb_3 distribution within detergent resistant membranes (DRM) modulates VT cell cytotoxicity (3, 4). Although the variants VT1 and VT2 both bind Gb_3 (1, 2), VT2 is more frequently associated with disease (5, 6), and differential VT1/VT2 Gb_3-containing DRM binding has been recently reported (7). GSLs have extensive fatty acid heterogeneity of unknown function, and the aglycone can markedly affect receptor function (8). VT-Gb_3 binding is affected by the fatty acid chain length, hydroxylation, degree of unsaturation (9–12), membrane phospholipid (13), and sterol (7, 14) composition. Gb_3 fatty acid composition influences intracellular VT1 trafficking (15), and it is intuitive that lipid structure influences GSL-raft partitioning (16). Gb_3 is also involved in HIV infection. The V3 loop of the HIV adhesin gp120 binds several GSLs (17, 18), including Gb_3 (19), and a soluble Gb_3 mimic inhibits infection and membrane fusion (20). We have proposed Gb_3 as a resistance factor against HIV infection (21, 22).

Using a novel in vitro assay (23) to construct simple DRMs from Gb_3 and cholesterol and the Langmuir monolayer surface pressure balance (24), we investigated the effect of Gb_3 fatty acid content on ligand (VT1, VT2, gp120) Gb_3 binding. We find a surprising dominant effect of fatty acid composition on Gb_3 availability for ligand/DRM binding with a single methylene transition.

MATERIALS AND METHODS

Materials

VT1 and VT2 were purified as described (25). Gb_3 was purified from human kidney (10). Horseradish peroxidase (HRP)-conjugated goat anti-rabbit was purchased from Sigma. Cholesterol and sphingomyelin were from Sigma. R5 HIV gp120 and Mab anti gp120 were from the NIH AIDS Research and Reference Reagent Program (Rockville, MD).

Gb_3 fatty acid isoforms

The fatty acid composition of purified renal Gb_3 was determined by FAB MS. Gb_3 homologs corresponding to these fatty

Abbreviations: Chol, cholesterol; DRM, detergent resistant membrane; Gb_3, globotriaosyl ceramide; GSL, glycosphingolipid; SM, sphingomyelin; VT, verotoxin

[1]To whom correspondence should be addressed.
    email: cling@sickkids.ca

This article is available online at http://www.jlr.org

acid isoforms were made by deacylation of renal Gb_3 and reacylation of lyso-Gb_3 with a single fatty acid as previously described (9).

Labeling of verotoxin

^{125}I VT1 and ^{125}I VT2 were prepared using Iodogen (Pierce) under conditions previously described (26), which have no effect on Gb_3 binding or cell cytotoxicity.

Gb_3/cholesterol DRM construction

Gb_3/cholesterol DRM were generated as described (23). Briefly, a 2:1 ratio of Gb_3 (50 µg) and cholesterol (25 µg) in ethanol were dried together and dissolved in 750 µl of MES-Triton buffer (25 mM MES, 150 mM NaCl pH 7.2, 1% Triton X-100). The solution was vortexed (1 min), sonicated (1 min), heated at 55°C (5 min) and vortexed (1 min). Then 750 µl of 70% sucrose solution in MES (pH 7.2) was added, gently mixed, and allowed to stand at room temperature for about 1 h. The mixture was then placed below 1 ml of 30% sucrose containing 1 µg.ml^{-1} ^{125}I-VT1. This was then overlaid successively with 1 ml of 30% sucrose and 1.5 ml of 5% of sucrose and condensed lipid species separated by floatation ultracentrifugation at 14,000 g for 72 h at 20°C. Although cell DRM are often isolated at 4°C, we found that separation was not altered at room temperature. From the top of the tube, 10 fractions, 500 µl each, were collected and counted in a γ−counter.

Immunoblot analysis of DRM fractions

Aliquots of the gradient fractions were loaded on to nitrocellose using a Slotblot apparatus (Shliecher and Schuell Minifold I microsample filtration manifold). The samples were washed with 50 mM TBS, 150 mM NaCl containing 1% skim milk blocking solution and left at 37°C for 1 h. The membrane was rinsed with TBS and incubated with anti gp120-Mab F425 B4a1 or Mab anti VT1 (1µg/ml), as appropriate, for 2 h at room temp. After washing, bound antibody was detected using an appropriate HRP conjugated anti-species antibody.

Langmuir trough monolayer surface pressure

The surface pressure was measured with a fully automated microtensiometer (µTROUGH S, Kibron Inc., Helsinki, Finland). The apparatus allowed the recording of the kinetics of interaction of a ligand with the monomolecular film using a set of specially designed Teflon troughs. All experiments were carried out in a controlled atmosphere at 23°C ± 0.5°C. Monomolecular films of Gb_3 or Gb_3 analogs (1-2µg) ± cholesterol were spread on pure water subphases (400 µl) from hexane/chloroform/ethanol solution as described previously (24, 27). After spreading the film, 5 min was allowed for solvent evaporation. To measure the interaction of VT1, VT2 or gp120 with Gb_3 monolayers, the ligand was injected in the subphase with 10 µl Hamilton syringe, and pressure increases produced were recorded for the indicated time. The data were analyzed with the Filmware version 3.57 program (Kibron Inc., Finland). The accuracy of the system under our experimental conditions was ± 0.25 mN.m^{-1} for surface pressure.

DRM gradient binding to C16Gb_3 (□), C17Gb_3 (◇), C18Gb_3 (■), C20Gb_3 (◆), C22Gb_3 (●) and C24Gb_3 (△). (ii) TLC/orcinol stain of GSL extract of control renal Gb_3 fractions. (B) Effect of fatty acid α-hydroxylation. C18Gb_3 (△), C22Gb_3 (◆), OHC18 Gb_3 (□), OHC22 Gb_3 (■). (C) Effect of fatty acid unsaturation. C24Gb_3 (●) and C24:1Gb_3 (▲). (D) ^{125}I-VT2 binding profile to Gb_3/chol DRM formed by (○) renal, (◆) C18Gb_3. In all cases, native renal Gb_3 (○) is control. DRM, detergent resistant membrane; Gb_3, globotriaosyl ceramide; VT, verotoxin.

Fig. 1. Effect of Gb_3 fatty acid content on the binding of ^{125}I-VT1 to Gb_3/cholesterol DRMs. (1i) Mass spectrometry analysis of human renal Gb_3. Only the Gb_3 mass range is shown. The masses highlighted are the sodium adducts of Gb_3 containing the indicated fatty acid. (1ii) ^{125}I-VT1 binding profile to Gb_3/chol DRMs formed by different isoforms of Gb_3. (A) Effect of chain length. (i)

TABLE 1. Summary of VT1/VT2 Gb$_3$ isoform DRM binding

Gb$_3$	VT1	VT2
Native Gb$_3$	100%	100%
C16 Gb$_3$	57.5 ± 17.7	108.9 ± 12.6
C18 Gb$_3$	53 ± 0.6	81.6 ± 2.3
C20 Gb$_3$	4.2 ± 1.4	52.1 ± 3.0
C22 GbGb$_3$	70 ± 21.2	213.5 ± 19.1
C24 Gb$_3$	48.3 ± 15.3	69.5 ± 8.5
C24:1 Gb$_3$	48.8 ± 15.9	36 ± 1.4
Mixture w/o C24:1 Gb$_3$	4.3 ± 3.8	73.5 ± 4.9
Mixture +C24:1 Gb$_3$	100 ± 0.0	75 ± 0.0

RESULTS

Gb$_3$ fatty acid chain content effects

VT1 binding to Gb$_3$/cholesterol DRM constructs. Human renal Gb$_3$ comprises C16 (21%), C18 (5%), C20 (9%), C22 (15%), C24 (27%), and C24:1 (23%) fatty acids (**Fig. 1i**). Accordingly, these isoforms were synthesized from lyso-Gb$_3$ and assessed for model DRM VT binding.

The ^{125}I-VT1/Gb$_3$ DRM gradient profiles (Fig. 1ii) show VT1 was bound only in fraction 1 (± fraction 2). Gb$_3$/cholesterol DRMs containing C16 fatty acid showed 75% binding compared with renal Gb$_3$. Surprisingly, no VT1 binding to either C18 or C20 fatty acid Gb$_3$ DRM (6.6% and 3%, respectively) was observed (**Table 1**). No VT1 bound to the nonphysiological C17Gb$_3$ either. Longer chain fatty acid Gb$_3$ DRMs (C22 and C24) showed about 75% and 50% binding, respectively. α-Hydroxylation of C18Gb$_3$ had no effect on VT1 binding. In contrast, α-hydroxylation of C22Gb$_3$ dramatically decreased the binding to Gb$_3$ DRMs [Fig. 1ii(B)]. Fatty acid unsaturation did not significantly affect the binding profile [Fig. 1ii(C); cf. 24:0 versus 24:1]. In contrast, VT2 bound C18/C20Gb$_3$ DRMs very well [Fig. 1ii(D) and Table 1]. In all cases, no binding to the gradient fraction containing most Gb$_3$ (fraction 5) [Fig. 1ii(A)(ii)] was seen, and this has been studied separately (Mahfoud, R., A. Manis, C. Ackerley, and C. Lingwood, unpublished observations). The nature of the fatty acid only affected binding to the Gb$_3$ DRMs at the gradient top (fraction 1 ± 2).

VT1-DRM binding to mixed Gb$_3$ DRMs

VT1 binding to in vitro reconstituted Gb$_3$ was initially addressed by mixing the different Gb$_3$ fatty acid isoforms [C16 (27%) + C18 (11%) + C20 (11%) + C22 (18%) + C24 (33%)] according to the composition of renal Gb$_3$ (Fig. 1i). Due to the tendency of unsaturated fatty acid containing GSL to be excluded from DRM (28–31), C24:1Gb$_3$ was not initially included. **Fig. 2A** compares the binding profile of ^{125}I-VT1 to renal Gb$_3$ (considered as control) to a corresponding Gb$_3$ mixture. Surprisingly, there was no significant VT1/DRM binding. Then we removed the individually VT1 unbound Gb$_3$ species. VT1 binding was significantly augmented upon removal of the C18 isoform (200% control; Fig 2B). Removal of C20 had a lesser, but significant, effect (100% control; Fig. 2B). Addition of α-hydroxylated C18 increased VT1 binding and addition of α-hydroxylated C22 showed 100% control binding (Fig. 2C).

Counter to the perceived incompatibility of unsaturation with "raft" formation, when we added the missing

C24:1Gb$_3$ to the mixture [C16 (21%) + C18 (5%) + C20 (9%) + C22 (15%) + C24 (27%) + C24:1 (23%)], a significant increase in binding was seen (100% control; Fig. 2D). The ^{125}I-VT1 profile of the mixture could now be superimposed on that of native renal Gb$_3$. In binary Gb$_3$ DRM constructs, C24:1 increased VT1 binding and countered C18 and C20Gb$_3$ (**Table 2**).

These studies indicate that the individual Gb$_3$ fatty acid isoforms form a balance within these fraction 1 Gb$_3$/cholesterol-DRM to promote or prevent VT1 recognition. However, for fraction 5 DRM, Gb$_3$ is not recognized, irrespective of fatty acid content.

Modulation of VT1 recognition of Gb$_3$ fatty acid isoform DRMs

For fatty acid species not bound by VT1, the Gb$_3$ distribution was not different from VT1-bound Gb$_3$ fatty acid isoforms (**Fig. 3**). The inhibitory effect seen with C18 and C20Gb$_3$/cholesterol DRMs raised the question whether C18 and C20Gb$_3$ could generate VT1 binding DRMs without cholesterol. In absence of cholesterol, C18Gb$_3$ was capable of forming fraction 1 DRMs bound by VT1 [Fig. 3A(i)], but the Gb$_3$ distribution in the gradient did not change. The fractions containing maximum C18Gb$_3$ [Fig. 3A(ii) and (iii)] still did not correspond to the ^{125}I-VT1 binding. For C20Gb$_3$, the lack of cholesterol did not enhance VT1 binding [Fig. 3B(i)]. However, inclusion of sphingomyelin (SM), considered as a key component of cell membrane lipid rafts (33, 34), dramatically increased ^{125}I-VT1 C20Gb$_3$ DRM binding [Fig. 3C(i)]. This was accompanied by a redistribution of Gb$_3$ in the gradient [Fig. 3C(ii)]. SM moved some C20Gb$_3$ from fractions 3–5 to fractions 1 and 2, corresponding to the binding peak of ^{125}I-VT1.

VT2 Gb$_3$ DRM binding is largely independent of fatty acid content

As shown in Table 1, fatty acid chain length did not affect VT2 binding to fraction 1 Gb$_3$/cholesterol DRM, as seen for VT1. VT2 more efficiently bound Gb$_3$ C22, and C16 DRM (227% and 118% renal control, respectively), but all fatty acid isoforms were bound by VT2. The saturated isoform mixture not bound by VT1 was bound by VT2, and addition of Gb$_3$ C24:1 to this in vitro reconstituted Gb$_3$ mixture did not affect VT2 binding. Nevertheless, no VT2 binding to fraction 5 DRM was observed.

HIV gp120 binding to Gb$_3$ fatty acid isoform DRMs mimics that of VT1

Gp120 binding within fraction 1 of single fatty acid isoform Gb$_3$/cholesterol DRMs was similar to VT1 (**Fig. 4**). There was efficient binding to C16Gb$_3$ DRMs, poor or no binding to C18 or C20Gb$_3$ DRMs, strong binding to C22Gb$_3$ DRMs, and reduced recognition of C24Gb$_3$ DRMs. In each case, no binding within fraction 5 DRM was seen.

HIV gp120 binding to mixed Gb$_3$ fatty acid isoform DRM mimics that of VT1

As for VT1, mixing the individual Gb$_3$ fatty acid isoforms to reconstitute the renal Gb$_3$ composition results in gp120
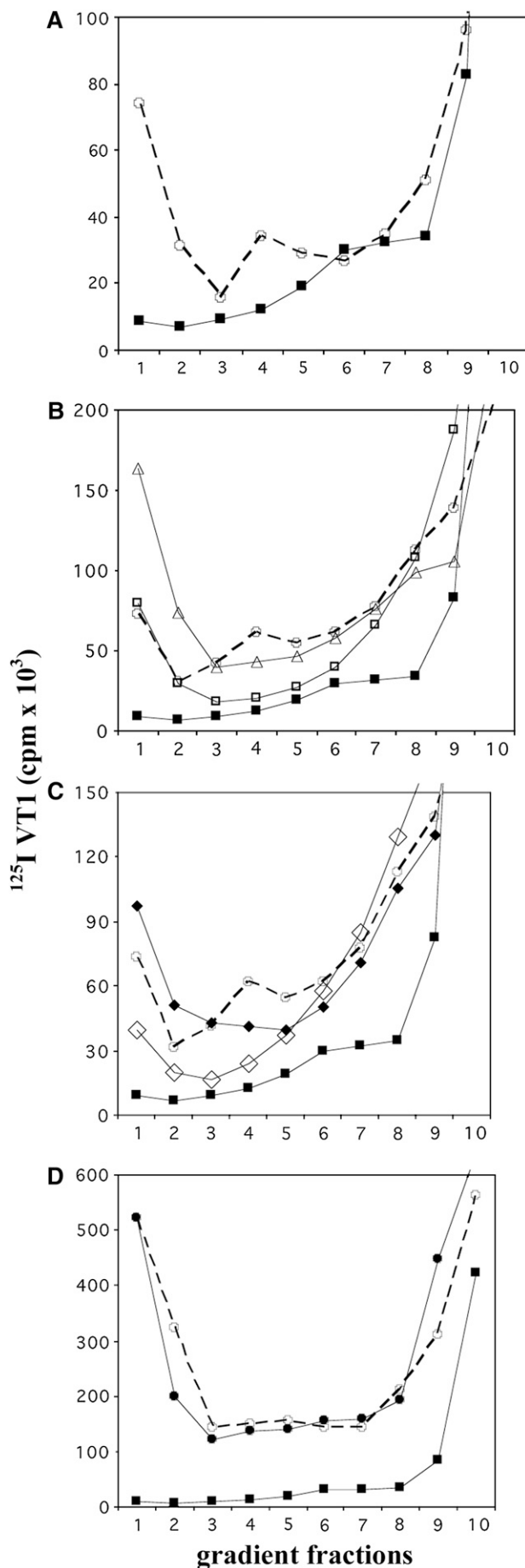
TABLE 2. Gb$_3$ isoform binary mixture DRM binding

Mixture	% of VT1 Binding
Control	100%
C16+C24:0 (1:1)	40%
C16+C24:0 (4:1)	60%
C16+C24:1 (1:1)	120%
C18+C24:1 (1:1)	100%
C20+C24:1 (1:1)	100%
C18+C20:0 (1:1)	65%

binding vesicles in fraction 1(**Fig. 5B**). As for VT1, omission of the C24:1Gb$_3$ results in the complete loss of binding (Fig. 5C). Removal of C18 or C20 from the C24:1 deficient mix had no effect (Figs. 5D and 5E), but removal of both induced gp120 binding (Fig. 5F). Mixing C18 and C24:1 fatty acid Gb$_3$s, which alone show no binding, generates gp120 binding DRMs (Fig. 5G).

Monolayer surface pressure shows unique profile for VT1 C18 and C20Gb$_3$

A Langmuir film balance was used to examine ligand binding to Gb$_3$ ± cholesterol. VT1 binding/insertion to renal Gb$_3$ monolayers showed a sigmoidal increase in surface pressure, enhanced in the presence of cholesterol [**Fig. 6i(A)** and **Table 3**]. The interaction was dose dependent (not shown) with a maximal surface pressure increase at 200 nM. Specificity of the VT-Gb$_3$ interaction was assessed by increasing the initial surface pressure (πi) to reduce the maximum surface pressure increase($\Delta\pi$ max). At a πi $\leq$ 30 mN/m, corresponding to a fluid disordered (l$_d$) phase, the $\Delta\pi$ max induced by VT1 was about 6 mN/m [Fig. 6i(A) and Table 2]. For values of πi greater than 30 mN/m, which correspond to raft-like liquid-ordered (l$_o$) phase domains (31), $\Delta\pi$ max gradually decreased as πi increased. This demonstrates the high specificity of the interaction as previously established for several other lipids and ligands (18, 34). The critical pressure of insertion (i.e., the theoretical value of πi extrapolated for $\Delta\pi$ max = 0 mN/m) was 42 mN/m. Interestingly, the mean lipid density of cellular membranes corresponds to a surface pressure of at least 30 mN/m (34).Thus, these data suggest that the interaction of VT1 with Gb$_3$ requires a densely packed organization of GSL, likely to occur within lipid rafts. However, VT2 could interact with renal Gb$_3$ only when the film was prepared at a low πi (less than 30 mN/m) (Fig. [6i(B)]). No interaction occurred at the physiological pressure of 30 mN/m and cholesterol had significantly less effect (Fig. 6i(B)] than for VT1.

Fig. 2. Binding of ^{125}I-VT1 to mixed isoform Gb$_3$ DRMs. (A) ^{125}I-VT1 binding profile to Gb$_3$/cholesterol DRM constructs. According to the mass spectrometry, Gb$_3$ was reconstituted in vitro by mixing the different species of Gb$_3$ = C16 (27%) + C18 (11%) + C20 (11%) + C22 (18%) + C24 (33%) (■). (B) ^{125}I-VT1 binding to mixture without C18 (△) or C20 (□). (C) ^{125}I-VT1 binding to mixture containing α-hydroxylated C18 (◇) or α-hydroxylated C22 (◆). (D) [125]I VT1 binding to mixture plus C24:1 (●). In all cases, renal Gb$_3$ (○) was positive and the mixture (■) negative control. DRM, detergent resistant membrane; Gb$_3$, globotriaosyl ceramide; VT, verotoxin.
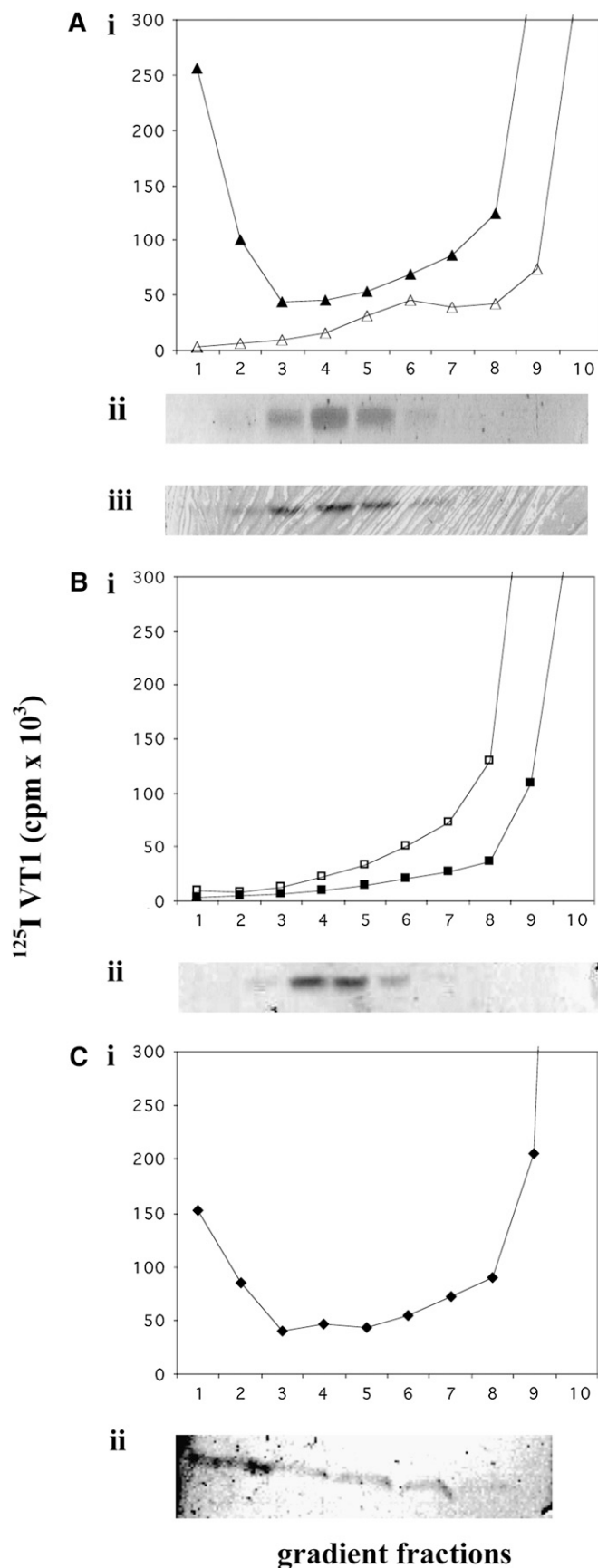
Fig. 3. Comparison of ^{125}I-VT1 binding to C18,C20Gb$_3$ DRMs ± cholesterol. (A) ^{125}I-VT1 and C18Gb$_3$ gradient distribution. (i) ^{125}I-VT1 gradient profile in presence (△) or absence (▲) of cholesterol.

VT1 efficiently bound C16 and C22Gb$_3$ [Fig. 6ii(A), Fig. 6ii(D), and Table 3]. However, for C18 and C20Gb$_3$ no specific binding was apparent [Figs. 6ii(B) and 6ii(C)]. The $\Delta\pi$ max was unaltered by increasing πi. However, with cholesterol, VT1 binding/insertion to C18 or C20Gb$_3$ was restored (Fig. 6 and Table 3). Thus, cholesterol fluidizes the C18/C20Gb$_3$ monolayer to allow VT1 insertion. In contrast, VT2 was found to bind both C16 and C18Gb$_3$ efficiently [Figs. 6ii(E) and 6ii(F)]. For these isoforms, especially C18Gb$_3$, VT2 is able to bind at high initial surface pressure (πi greater than 30 mN/m). Similarly VT2c, which is much more cytotoxic than VT1 or VT2 (26), bound C18 and C20Gb$_3$ monolayers very effectively (not shown). Gp120, however, showed no specific interaction with C18Gb$_3$ compared with C16 or renal Gb$_3$ monolayers [Figs. 6iii(A) and 6iii(B); cf. 6iii(C)], as for VT1, but gp120 retained specific C20Gb$_3$ binding [Fig. 6iii(D)]. The VT1/gp120 selective transition between C16 and C18Gb$_3$ corresponds to the loss of VT1 and gp120 (but not VT2) binding within the sucrose gradient Gb$_3$ DRM constructs. In this case, addition of the unsaturated C24:1Gb$_3$, also increasing fluidity, induced VT1 binding. Thus the lack of binding to C18 and C20Gb$_3$ may be due to excessive rigidity (order) the lateral interaction of these isoforms may achieve.

DISCUSSION

Resistance to cold detergent extraction is a common approach to the study of cellular lipid rafts (35) that are enriched in cholesterol and GSLs (36). Although DRMs represent a useful index of cell membrane architecture (37), the procedure does not result in membranes which reflect the original membrane organization (35), but rather an amalgam of originally potentially distinct domains. The GSL/cholesterol ratio (about 1.4) of our DRM vesicles represents a transition for micelle and vesicle formation (38) and is thus the simplest DRM system to study aglycone modulation of GSL receptors. These vesicles do not reflect the more complex lipid composition of cell DRMs, but they provide a manipulable analytical tool. To improve resolution, we centrifuged for longer than is typical for cell-derived DRMs and separated two vesicle populations, one at the gradient top which binds ligand and a second fraction of larger vesicles that remain ligand unbound (Mahfoud, R., A. Manis, C. Ackerley, and C. Lingwood, unpublished observations).

Our studies show two precise transitions in the Gb$_3$ fatty acid alkyl chain length which regulate carbohydrate presentation for ligand binding in this model DRM vesicle system. No VT1 or gp120 binding is seen between C17 and C20, either in the cholesterol vesicle constructs separated

(ii) C18Gb$_3$ gradient distribution in (▲). (iii) C18Gb$_3$ gradient distribution in (△). Gradient fractions were analyzed for C18Gb$_3$ content by TLC/orcinol. (B) ^{125}I-VT1 and C20Gb$_3$ gradient distribution. (i) ^{125}I-VT1 gradient profile with (■) or without (□) cholesterol. (ii) C20Gb$_3$ gradient distribution determined by TLC. (C) ^{125}I-VT1 (i) and C20Gb$_3$ gradient distribution with cholesterol + sphingomyelin (◆). (ii) C20Gb$_3$ gradient distribution in (◆).DRM, detergent resistant membrane; Gb$_3$, globotriaosyl ceramide; VT, verotoxin.
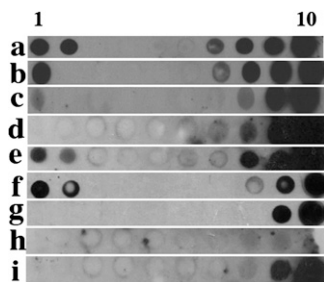
Fig. 4. R5 HIV gp120 binding to Gb$_3$ fatty acid isoform/cholesterol DRM constructs. Gb$_3$/cholesterol DRMs were separated on sucrose gradients in the presence of gp120. Aliquots of the fractions (1–10) were immobilized on nitrocellulose and gp120 detected immunochemically. (a) renal Gb$_3$; (b) C16Gb$_3$; (c) C18Gb$_3$; (d) C20Gb$_3$; (e) C22Gb$_3$; (f) C24Gb$_3$; (g) C24:1Gb$_3$; (h) renal Gb$_3$ w/o gp120; (i) Gb$_4$ DRMs. DRM, detergent resistant membrane; Gb$_3$, globotriaosyl ceramide; VT, verotoxin.

on a sucrose gradient or in water/air interface monolayers. This is not an exclusion of Gb$_3$ carbohydrate for ligand binding, for in each case, VT2 binding is largely unaffected. By TLC overlay, each of the Gb$_3$ isoforms is effectively bound by both VT1 and VT2.

This C16/C17 Gb$_3$ alkyl chain transition is similar to that reported for saturated phospholipid/cholesterol bilayer interaction (39). Cholesterol matches the dimensions of C16 alkyl chain to reduce PC alkyl chain tilt, whereas the overlap of C18 deformed the PC/cholesterol bilayer structure. Cholesterol stabilizes the gel phase to increase the transition temperature for PC alkyl chain length <C17 but destabilizes to decrease transition temperature for fatty acids >C18 (40), although species longer than C20 were not assessed. This transition approximates to the 20Å long axis of cholesterol. However both alkyl chains were homologous, whereas in our studies the sphingosine remains constant. Our finding essentially the same transition, indicates cholesterol–fatty acid mismatch provides the basis of Gb$_3$ fatty acid dependent receptor function. Phospholipid fatty acid unsaturation decreases interaction with cholesterol (41) consistent with the dominant positive effect of C24:1Gb$_3$ we observed.

As for other GSLs, the lipid moiety of Gb$_3$ is heterogeneous in fatty acid chain length, α-hydroxylation, and un-
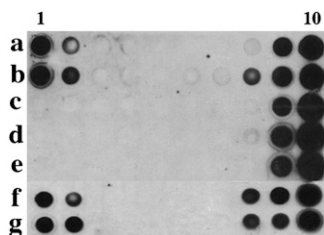
Fig. 5. Binding of gp120 to mixed isoform Gb$_3$ DRMs. Gp120 was included in gradients separating Gb$_3$/cholesterol DRMs. (a) renal Gb$_3$; (b) mix of Gb$_3$ fatty isoforms corresponding to renal Gb$_3$; (c) Gb$_3$ mix without C24:1; (d) Gb$_3$ mix without C24:1 and C18; (e) Gb$_3$ mix without C24:1 and C20; (f) Gb$_3$ mix without C24:1, C18, and C20; (g) C18 and C24:1Gb$_3$ only. DRM, detergent resistant membrane; Gb$_3$, globotriaosyl ceramide; VT, verotoxin.

saturation. Using a cholesterol/PC/Gb$_3$ ELISA, increasing fatty acid chain length (from C16 to C24) and unsaturation promoted VT1 binding (9) and differentially affected the binding of VT1 and VT2c in solid phase assays (9, 11). Our evidence has indicated that such changes are also important in VT1/VT2 binding to Gb$_3$ within the human renal glomerulus (14). The lipid moiety itself is crucial to the verotoxin receptor function of Gb$_3$ as the lipid-free sugar shows little VT binding (42–44). In addition to VT binding, intracellular routing of the toxin Gb$_3$ complex within cells correlates with the lipid moiety (15). After multivalent binding to Gb$_3$ receptors, VT1 (and VT2) (7) is internalized via receptor-mediated endocytosis by both clathrin (45, 46) and caveolar (47–49) mediated mechanisms. Then the toxin follows a retrograde transport route to the Golgi apparatus and endoplasmic reticulum (ER) (15, 46, 50–52) where the A subunit is translocated to the cytosol to inhibit protein synthesis (7). Despite equivalent Gb$_3$ expression, cells with higher levels of shorter fatty acid (C16:0,C18) containing Gb$_3$ were significantly more sensitive to VT1 compared with a cell line with higher levels of longer fatty acid (C24:0) Gb$_3$ content (53). VT1 was directed only to the Golgi region in less sensitive cells while within the same time frame, retrograde transport of VT1 to ER and nuclear membrane took place in highly sensitive cells (15, 53). We proposed that Gb$_3$ isoforms with long chain fatty acids preferentially remain in the plasma membrane, whereas short chain fatty acid Gb$_3$ isoforms are preferentially internalized to mediate retrograde transport and VT1 cytotoxicity. VT1 B subunit within this pathway remains within the DRM fraction in sensitive cells but is found within the non-DRM fraction in Gb$_3$ positive, VT resistant cells in which internalized toxin is trafficked to the lysosome (3, 54). However, although DRM and non-DRM Gb$_3$ may be differentially trafficked within the cell, this does not provide the basis for retrograde transport. Gb$_3$ DRM binding is essential for VT cytotoxicity via ER cytosolic translocation (4). Surprisingly, dissociation from DRMs did not affect VT1 retrograde transport to the Golgi/ER (4). VT1 internalization alters the subsequent plasma membrane Gb$_3$ content during a long lasting recovery phase (55), suggesting that a particular Gb$_3$ assembly is internalized by VT and trafficked to the ER. VT1 and VT2 bind both shared and distinct cell surface domains which remain distinct/common during internalization and retrograde transport. Unlike VT1, much of VT2 binds and is internalized with transferrin but intracellular VT1 and VT2 transport coalesce at the Golgi (7). Cell bound VT1 is more detergent resistant than VT2 and binding to cell derived or in vitro constructed Gb$_3$ DRMs is more significant for VT1 (7). This correlates with our current monolayer studies which show VT1, but not VT2, is able to bind and insert in to Gb$_3$ monolayers at surface pressures corresponding to liquid ordered domains. Increased cholesterol inhibited VT1 (but not VT2) Gb$_3$ DRM binding and sphingomyelin preferentially augmented VT2 Gb$_3$ DRM binding (7). Thus these toxin homologs bind different Gb$_3$ lipid assemblies.

Though the affinity for Gb$_3$ binding by VT2 is less than that of VT1, it is clear from renal tissue (14) and fraction 1 Gb$_3$ DRM binding, that VT2 is less restrictive as to the lipid

context in which Gb₃ is recognized. That this VT1 restriction is shared by HIV gp120, suggests that this is a significant, rather than subtle, conformational difference. Gb$_3$ has been implicated both as a cofactor for gp120 (56) and as a resistance factor against HIV (21, 22) and gp120-GSL binding is modulated by the lipid moiety (57).

In the present experiments, we studied the effect of the Gb$_3$ fatty acid chain length, α-hydroxylation and unsaturation on the binding of VT to Gb$_3$ DRMs. Early studies showed that C16, C18, C22, C24 and C24:1 fatty acids were the most common species in all the GSL fractions of human kidney (58). Our analysis of the human kidney showed similar results (10, 14). Hydroxylated fatty acids were only a minor component (10, 14). The basis of cellular GSL fatty acid heterogeneity lies at the level of ceramide synthase, since several fatty acid selective ceramide synthase isoforms have been defined (59, 60). In our model studies, Gb$_3$ C16 and C22 showed the best DRM binding for both VT1 and VT2. No binding was seen for VT1 (or gp120) with the intermediate isoforms (C17, C18 and C20), but these Gb$_3$ DRMs were effectively bound by VT2. This fatty acid modulation of carbohydrate presentation is separate from the lack of GSL carbohydrate ligand binding we have found within the major GSL/cholesterol vesicle fraction (Mahfoud, R., A. Manis, C. Ackerley, and C. Lingwood, unpublished observations) but the principles we observe provide insight in to the basis of membrane regulation of GSL receptors. As for native Gb$_3$ (Mahfoud, R., A. Manis, C. Ackerley, and C. Lingwood, unpublished observations), gradient DRM vesicles at the 5/30% sucrose interface (the classical 'raft' fraction) were not bound by any ligand for any Gb$_3$ fatty acid isoform or mixture thereof.

Our evidence indicates that within Gb$_3$/cholesterol DRMs, a mere 1-carbon difference within the Gb$_3$ acyl chain can act as a "switch" to define VT1 (and gp120) binding. The presence of a single isoform within a mixture can determine maximum or minimum binding.

We reconstituted a mixture of Gb$_3$ fatty acid isoforms in vitro according to mass spectrometry analysis of the human renal Gb$_3$ fraction. Initially we omitted the only unsaturated species (C24:1). Unsaturation has been generally considered unfavorable for raft formation (61). Indeed, C24:1Gb$_3$/cholesterol was very poorly/not bound by VT1 and gp120. However, no binding of VT1/gp120 was seen to the mixture of saturated fatty acid Gb$_3$ isoforms either. The removal of C18Gb$_3$, which alone did not bind VT1 in our system, dramatically increased VT1 binding. Despite its minimal presence in the mixture, C18Gb$_3$ determines the VT1/Gb$_3$ binding in a dominant negative manner. Removal of C20, which is also unable to support VT1 binding alone, was also sufficient to induce VT1 binding to the saturated isoform mixture, suggesting C18 and C20Gb$_3$ have an additive negative effect on VT1 Gb$_3$/cholesterol binding. For gp120, removal of both C18 and C20Gb$_3$ was required to allow binding. Addition of the C24:1 isoform to any mixture of saturated isoforms induced VT1 recognition. Thus C24:1 counteracts the inhibitory effects of C18 and C20Gb$_3$. Adding both C24:1 and, for example, C18Gb$_3$, neither of which bind VT1 or gp120 alone, induces extensive VT1 and gp120 DRM binding. This is a remarkable property whereby GSL fatty acid isoforms, which show no receptor function, when combined are strongly bound, and it suggests that a balance between rigid and fluid structures optimizes membrane GSL receptors.

Fatty acid α-hydroxylation shows an effect similar to C24:1. In the single Gb$_3$ isoform format, hydroxylation inhibited VT1 binding (C22 c.f. C22OH), but if an hydroxylated isoform is added to a mixture of other isoforms for which no DRM binding is seen, DRM binding is significantly increased. αHydroxylation can mediate H-bonding with GSL headgroups (62), but the effect on cholesterol interaction has yet to be reported. GSL fatty acid hydroxylation may decrease fluidity in a homogeneous system but disturb packing in a mixture to increase
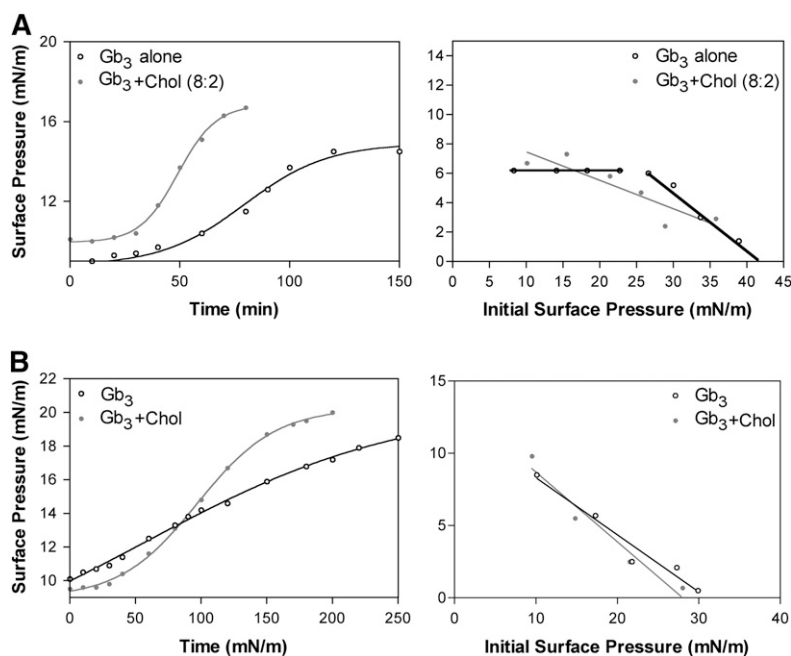
Fig. 6. Air/water monolayer insertion assay of VT1, VT2, and gp120 Gb$_3$ binding. Ligand binding/insertion in Gb$_3$ monolayers ±cholesterol were measured using a Langmuir trough. Left panels indicate time course; right panels indicate increasing initial pressure (6i) renal Gb$_3$ A:VT1, B:VT2. (6ii) A: VT1 and C16Gb$_3$; B: VT1 and C18Gb$_3$ (specific binding for C18:2Gb$_3$ is also shown); C: VT1 and C20Gb$_3$; D: VT1 and C22Gb$_3$; E: VT2 and C16 Gb$_3$; F: VT2 and C18 Gb$_3$. (6iii) A: gp120 and renal Gb$_3$; B: gp120 and C16Gb$_3$; C: gp120 and C18Gb$_3$; D: gp120 and C20Gb$_3$. VT1 and gp120 both show a selective loss of specific binding for C18Gb$_3$ monolayers. DRM, detergent resistant membrane; Gb$_3$, globotriaosyl ceramide; VT, verotoxin.
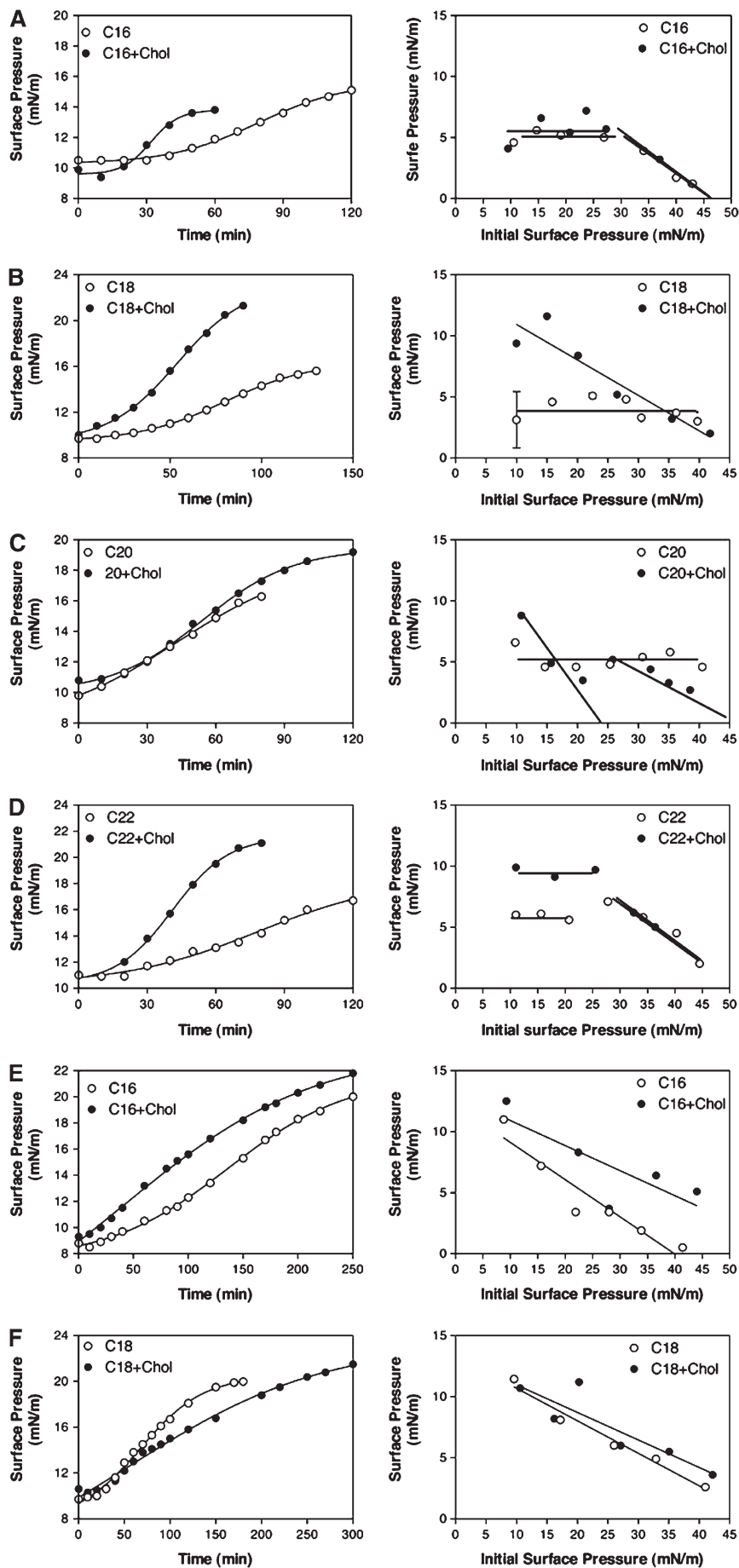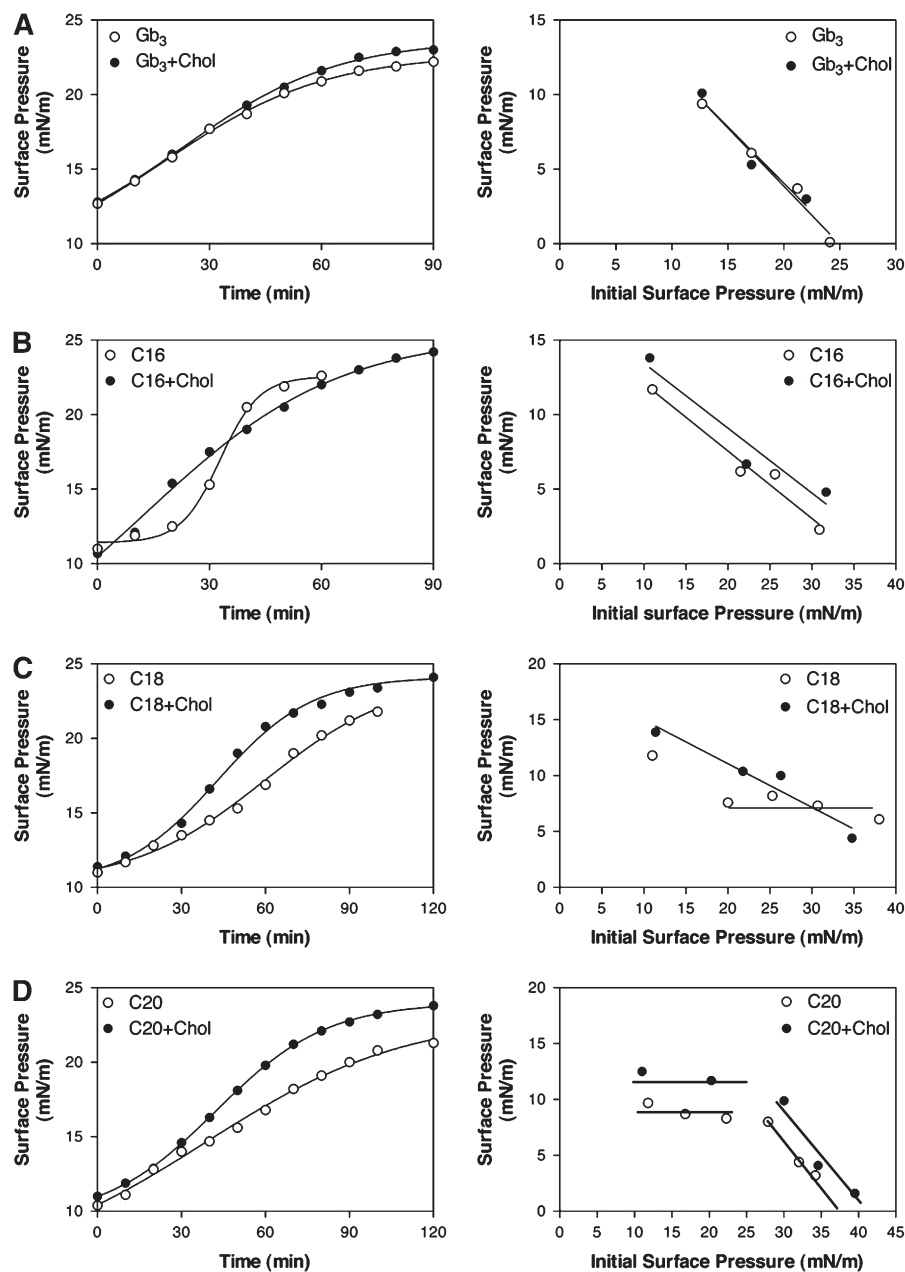
Fig. 6.—*Continued.*

Fig. 6.—*Continued.*

fluidity similar to C24:1. Consistent with this, mixing C24:1Gb$_3$ with C22OH Gb$_3$, neither of which shows DRM binding alone, does not induce VT1 binding. This is in stark contrast to mixing C24:1Gb$_3$ with C18Gb$_3$. Thus the "availability" of Gb$_3$ for VT1 binding within cholesterol complexes is a balance between negative influence (C18, C20) and counter-balancers (C24:1, C18OH, C22OH),

despite the fact that these counter-balancers do not alone form VT1 bound DRM complexes. We propose that GSL receptor function within liquid-ordered, cholesterol-enriched microdomains requires a degree of fluidity. This fluidity may allow sufficient headgroup spacing to accommodate VT1/gp120 recognition. Gb$_3$ with fatty acids that most closely match the dimensions of conjugated ring system

TABLE 3. Surface pressure parameters for VT1/VT2 Gb$_3$ isoform monolayer binding/insertion

	Gb3 Alone								Gb3 + Chol (8:2)								
	Renal Gb3		Gb3 C16		Gb3 C18		Gb3C20	Gb3C22	Renal Gb3		Gb3 C16		Gb3 C18		Gb3C20	Gb3C22
	VT1	VT2	VT1	VT2	VT1	VT2	VT1	VT1	VT1	VT2	VT1	VT2	VT1	VT2	VT1	VT1
Vi (mN/m)	0.083	0.035	0.06	0.06	0.075	0.07	0.085	0.05	0.165	0.085	0.15	0.06	0.18	0.06	0.112	0.205
Äδ Max (mN/m)	7.1	8.5	4.6	11	5.43	11.45	6.6	6	6.7	9.8	4.1	12.5	10.75	10.9	8.8	9.9
Critical pressure of insertion (mN/m)	42	30	45	40	Non specific	50	Non specific	50	45	<30	45	>50	45	50	45	50

of cholesterol (C17, C18, C20) form a lipid domain too rigid to permit VT1/gp120 binding. These isoforms might sequester the cholesterol to explain their dominant negative effect.

It is clear that the Gb_3 fatty acid dependency of VT1 DRM binding is shared by gp120. Both C18 and $C20Gb_3$ DRMs are not bound. Isoform mixing shows very similar effects for VT1 and gp120. Although $C24:1Gb_3$ shows little (VT1) or no (gp120) binding, addition in mixes is dominate positive for binding. In the absence of $C24:1Gb_3$, $C18Gb_3$ and $C20Gb_3$ are dominant negative for binding both ligands. Removal of either will allow VT1 binding, but both must be removed to allow gp120 recognition.

The Langmuir trough monolayer studies verified the $C18Gb_3$ cut off for VT1 and gp120 but not VT2 binding, found in the DRM constructs. However in this assay, the lack of binding is seen without, rather than with, cholesterol. In addition, gp120 specific binding to $C20Gb_3$ was seen in monolayers but not for Gb_3 DRM vesicles. This difference may reflect the radius of curvature of the DRM bilayer/monolayer and that monomeric gp120 requires less fluidity since lateral pentamer accommodation is unnecessary. Although cholesterol/GSL membranes are more ordered than cholesterol/glycerolipid membranes, pure sphingolipids would form a gel ("solid") phase, which cholesterol converts to the liquid ordered (l_o) phase (63). Cholesterol intercalation will thus fluidize a pure GSL monolayer; C18 and $C20Gb_3$ monolayers may be too rigid to allow VT1/gp120 binding and insertion. Such rigidity could result from the approximate parity of the chain length of these fatty acids compared with the C18 sphingoid base. In fraction 1 DRM vesicles, the small radius of curvature may sufficiently reduce GSL/cholesterol bilayer order (64) to allow ligand binding. The Gb_3 fatty acid independence of VT2 binding in both DRMs and monolayers suggests that Gb_3 flexibility/fluidity is less restrictive for VT2 recognition than for VT1 and gp120.

Surface pressures which allow VT1 binding (greater than 30mN/m) are consistent with liquid ordered bilayer binding for VT1, but VT2 and gp120 only bind Gb_3 at lower surface pressures, consistence with "non-raft" membrane Gb_3 binding. This is consistent with the lower Gb_3 DRM binding of VT2 we have reported (7) and with gp120 cell binding (in progress). However some individual Gb_3 fatty acid homologs show VT2 binding above 30mN/m.

The membrane receptor function of GSL is very complex. Our model studies provide a new investigational tool. The dominant positive effect of $C24:1Gb_3$ on DRM binding and the remarkable transitions between C16 and $C22Gb_3$ argue that a degree of fluidity within a raft is necessary for VT1 (or gp120) binding. Increasing the C24:1 content (but not to homogeneity) promotes ligand binding. In phosphatidylcholine and cholesterol, unsaturation of the Gb_3 fatty acid also increased VT1 binding (9). Due to the tendency of unsaturated fatty acid containing GSL to be excluded from lipid rafts (28, 30, 31, 65), these results were not anticipated.

The fatty acid dependent regulation of GSL receptor function may provide a physiological basis for the fatty acid selective dihydroceramide synthases (60).🍑

REFERENCES

1. Lingwood, C. A. 1993. Verotoxins and their glycolipid receptors. *In* Sphingolipids. Part A: Functions and Breakdown Products. Advances in Lipid Research. R. Bell, Y. A. Hannun, and A. Merrill Jr., editors. Academic Press, San Diego. 189–212.
2. Okuda, T., N. Tokuda, S. Numata, M. Ito, M. Ohta, K. Kawamura, J. Wiels, T. Urano, O. Tajima, and K. Furukawa. 2006. Targeted disruption of Gb3/CD77 synthase gene resulted in the complete deletion of globo-series glycosphingolipids and loss of sensitivity to verotoxins. *J. Biol. Chem.* **281:** 10230–10235.
3. Falguieres, T., F. Mallard, C. Baron, D. Hanau, C. Lingwood, B. Goud, J. Salamero, and L. Johannes. 2001. Targeting of Shiga toxin b-subunit to retrograde transport route in association with detergent-resistant membranes. *Mol. Biol. Cell.* **12:** 2453–2468.
4. Smith, D. C., D. J. Sillence, T. Falguieres, R. M. Jarvis, L. Johannes, J. M. Lord, F. M. Platt, and L. M. Roberts. 2006. The association of Shiga-like toxin with detergent-resistant membranes is modulated by glucosylceramide and is an essential requirement in the endoplasmic reticulum for a cytotoxic effect. *Mol. Biol. Cell.* **17:** 1375–1387.
5. Boerlin, P., S. A. McEwen, F. Boerlin-Petzold, J. B. Wilson, R. P. Johnson, and C. L. Gyles. 1999. Associations between virulence factors of Shiga toxin-producing Escherichia coli and disease in humans. *J. Clin. Microbiol.* **37:** 497–503.
6. Miceli, S., M. A. Jure, O. A. de Saab, M. C. de Castillo, S. Rojas, A. P. de Holgado, and O. M. de Nader. 1999. A clinical and bacteriological study of children suffering from haemolytic uraemic syndrome in Tucuman, Argentina. *Jpn. J. Infect. Dis.* **52:** 33–37.
7. Tam, P., R. Mahfoud, A. Nutikka, A. Khine, B. Binnington, P. Paroutis, and C. Lingwood. 2008. Differential intracellular trafficking and binding of verotoxin 1 and verotoxin 2 to globotriaosylceramide-containing lipid assemblies. *J. Cell. Physiol.* **216:** 750–763.
8. Lingwood, C. A. 1996. Aglycone modulation of glycolipid receptor function. *Glycoconj. J.* **13:** 495–503.
9. Kiarash, A., B. Boyd, and C. A. Lingwood. 1994. Glycosphingolipid receptor function is modified by fatty acid content: Verotoxin 1 and verotoxin 2c preferentially recognize different globotriaosyl ceramide fatty acid homologues. *J. Biol. Chem.* **269:** 11138–11146.
10. Pellizzari, A., H. Pang, and C. A. Lingwood. 1992. Binding of verocytotoxin 1 to its receptor is influenced by differences in receptor fatty acid content. *Biochemistry.* **31:** 1363–1370.
11. Binnington, B., D. Lingwood, A. Nutikka, and C. Lingwood. 2002. Effect of globotriaosyl ceramide fatty acid hydroxylation on the binding by verotoxin 1 and verotoxin 2. *Neurochem. Res.* **27:** 807–813.
12. Romer, W., L. Berland, V. Chambon, K. Gaus, B. Windschiegl, D. Tenza, M. R. Aly, V. Fraisier, J. C. Florent, D. Perrais, et al. 2007. Shiga toxin induces tubular membrane invaginations for its uptake into cells. *Nature.* **450:** 670–675.
13. Arab, S., and C. A. Lingwood. 1996. Influence of phospholipid chain length on verotoxin/globotriaosyl ceramide binding in model membranes: comparison of a surface bilayer film and liposomes. *Glycoconj. J.* **13:** 159–166.
14. Chark, D., A. Nutikka, N. Trusevych, J. Kuzmina, and C. Lingwood. 2004. Differential carbohydrate epitope recognition of globotriaosyl ceramide by verotoxins and monoclonal antibody: role in human renal glomerular binding. *Eur. J. Biochem.* **271:** 405–417.
15. Arab, S., and C. Lingwood. 1998. Intracellular targeting of the endoplasmic reticulum/nuclear envelope by retrograde transport may determine cell hypersensitivity to Verotoxin: sodium butyrate or selection of drug resistance may induce nuclear toxin targeting via globotriaosyl ceramide fatty acid isoform traffic. *J. Cell. Physiol.* **177:** 646–660.
16. Wang, T. Y., and J. R. Silvius. 2000. Different sphingolipids show differential partitioning into sphingolipid/cholesterol-rich domains in lipid bilayers. *Biophys. J.* **79:** 1478–1489.
17. Bhat, S., R. V. Mettus, E. P. Reddy, K. E. Ugen, V. Srikanthan, W. V. Williams, and D. B. Weiner. 1993. The galactosyl ceramide/sul-

fatide receptor binding region of HIV-1 gp120 maps to amino acids 206–275. *AIDS Res. Hum. Retroviruses.* **9:** 175–181.

18. Hammache, D., G. Piéroni, N. Yahi, O. Delézay, N. Koch, H. Lafont, C. Tamalet, and J. Fantini. 1998. Specific interaction of HIV-1 and HIV-2 surface envelope glycoproteins with monolayers of galactosylceramide and ganglioside GM3. *J. Biol. Chem.* **273:** 7967–7971.

19. Hammache, D., N. Yahi, M. Maresca, G. Pieroni, and J. Fantini. 1999. Human erythrocyte glycosphingolipids as alternative cofactors for human immunodeficiency virus type 1 (HIV-1) entry: evidence for CD4-induced interactions between HIV-1 gp120 and reconstituted membrane microdomains of glycosphingolipids (Gb3 and GM3). *J. Virol.* **73:** 5244–5248.

20. Lund, N., D. Branch, M. Mylvaganam, D. Chark, X. Ma, D. Sakac, B. Binnington, J. Fantini, A. Puri, R. Blumenthal, et al. 2006. A novel soluble mimic of the glycolipid globotriaosylceramide inhibits HIV infection. *AIDS.* **20:** 333–343.

21. Lund, N., M. L. Olsson, S. Ramkumar, D. Sakac, Y. Yahalom, C. Levene, A. Hellberg, X. Ma, B. Binnington, D. Jung et al. Protection against HIV-1 infection by the human P^k blood group antigen. Epub ahead of print. January 12, 2009; DOI 10.1182/blood-2008-03-143396.

22. Ramkumar, S., D. Sakac, B. Binnington, D. R. Branch, and C. A. Lingwood. 2009. Induction of HIV-1 resistance: cell susceptibility to infection is an inverse function of globotriaosyl ceramide levels. *Glycobiology.* **19:** 76–82.

23. Nutikka, A., and C. Lingwood. 2004. Generation of receptor active, globotriaosyl ceramide/cholesterol lipid 'rafts' in vitro: a new assay to define factors affecting glycosphingolipid receptor activity. *Glycoconj. J.* **20:** 33–38.

24. Mahfoud, R., M. Mylvaganam, C. A. Lingwood, and J. Fantini. 2002. A novel soluble analog of the HIV-1 fusion cofactor, globotriaosylceramide(Gb₃), eliminates the cholesterol requirement for high affinity gp120/Gb₃ interaction. *J. Lipid Res.* **43:** 1670–1679.

25. Nutikka, A., B. Binnington-Boyd, and C. A. Lingwood. 2003. Methods for the purification of Shiga toxin 1. *In* Methods in Molecular Medicine. D. Philpot and F. Ebel, editors. Humana Press, Totowa, NY. 187–195.

26. Head, S. C., M. A. Karmali, and C. A. Lingwood. 1991. Preparation of VT1 and VT2 hybrid toxins from their purified dissociated subunits: evidence for B subunit modulation of A subunit function. *J. Biol. Chem.* **266:** 3617–3621.

27. Mahfoud, R., M. Maresca, M. Santelli, A. Pfohl-Leszkowicz, A. Puigserver, and J. Fantini. 2002. pH-dependent interaction of fumonisin B1 with cholesterol: physicochemical and molecular modeling studies at the air-water interface. *J. Agric. Food Chem.* **50:** 327–331.

28. Rietveld, A., and K. Simons. 1998. The differential miscibility of lipids as the basis for the formation of functional membrane rafts. *Biochim. Biophys. Acta.* **1376:** 467–479.

29. Brown, D. A., and E. London. 1998. Structure and origin of ordered lipid domains in biological membranes. *J. Membr. Biol.* **164:** 103–114.

30. Pitman, M. C., F. Suits, A. D. Mackerell, Jr., and S. E. Feller. 2004. Molecular-level organization of saturated and polyunsaturated fatty acids in a phosphatidylcholine bilayer containing cholesterol. *Biochemistry.* **43:** 15318–15328.

31. Ali, S., H. Brockman, and R. Brown. 1991. Structural determinants of miscibility in surface films of galactosyl ceramide and phosphatidyl choline:effect of unsaturation in the galactosyl ceramide acyl chain. *Biochemistry.* **30:** 11198–11205.

32. Simons, K., and E. Ikonen. 1997. Functional rafts in cell membranes. *Nature.* **387:** 569–572.

33. Ait Slimane, T., and D. Hoekstra. 2002. Sphingolipid trafficking and protein sorting in epithelial cells. *FEBS Lett.* **529:** 54–59.

34. Maggio, B. 1994. The surface behavior of glycosphingolipids in biomembranes: a new frontier of molecular ecology. *Prog. Biophys. Mol. Biol.* **62:** 55–117.

35. Brown, D. A. 2006. Lipid rafts, detergent-resistant membranes, and raft targeting signals. *Physiology (Bethesda).* **21:** 430–439.

36. Kasahara, K., and Y. Sanai. 2000. Functional roles of glycosphingolipids in signal transduction via lipid rafts. *Glycoconj. J.* **17:** 153–162.

37. Lingwood, D., and K. Simons. 2007. Detergent resistance as a tool in membrane research. *Nature Protocols.* **2:** 2159–2165.

38. Hirai, M., M. Koizumi, H. Hirai, T. Hayakawa, K. Yuyama, N. Suzuki, and K. Kasahara. 2005. Structures and dynamics of glycosphingo-

39. McIntosh, T. J. 1978. The effect of cholesterol on the structure of phosphatidylcholine bilayers. *Biochim. Biophys. Acta.* **513:** 43–58.

40. McMullen, T. P., R. N. Lewis, and R. N. McElhaney. 1993. Differential scanning calorimetric study of the effect of cholesterol on the thermotropic phase behavior of a homologous series of linear saturated phosphatidylcholines. *Biochemistry.* **32:** 516–522.

41. Wassall, S. R., M. R. Brzustowicz, S. R. Shaikh, V. Cherezov, M. Caffrey, and W. Stillwell. 2004. Order from disorder, corralling cholesterol with chaotic lipids. The role of polyunsaturated lipids in membrane raft formation. *Chem. Phys. Lipids.* **132:** 79–88.

42. Boyd, B., Z. Zhiuyan, G. Magnusson, and C. A. Lingwood. 1994. Lipid modulation of glycolipid receptor function: presentation of galactose α1–4 galactose disaccharide for Verotoxin binding in natural and synthetic glycolipids. *Eur. J. Biochem.* **223:** 873–878.

43. Hilaire, N., A. Negre-Salvayre, and R. Salvayre. 1994. Cellular uptake and catabolism of high-density-lipoprotein triacylglycerols in human cultured fibroblasts: degradation block in neutral lipid storage disease. *Biochem. J.* **297:** 467–473.

44. Mylvaganam, M., B. Binnington, H. Hansen, G. Magnusson, and C. Lingwood. 2002. Interaction of verotoxin 1 B subunit with globotriaosyl ceramide analogues: Aminosubstituted (aminodeoxy) adamantylGb₃Cer provides insight into the nature of the Gb₃Cer binding sites. *Biochem. J.* **368:** 769–776.

45. Sandvig, K., S. Olnes, J. Brown, O. Peterson, and B. van Deurs. 1989. Endocytosis from coated pits of Shiga toxin: a glycolipid-binding protein from *Shigella dysenteriae* 1. *J. Cell Biol.* **108:** 1331–1343.

46. Khine, A. A., and C. A. Lingwood. 1994. Capping and receptor mediated endocytosis of cell bound verotoxin(Shiga-like toxin). 1: Chemical identification of an amino acid in the B subunit necessary for efficient receptor glycolipid binding and cellular internalization. *J. Cell. Physiol.* **161:** 319–332.

47. Schapiro, F., C. A. Lingwood, W. Furuya, and S. Grinstein. 1998. pH-independent targeting of glycolipids to the Golgi complex. *Am. J. Physiol.* **274:** 319–332.

48. Nichols, B., A. Kenworthy, R. Polishchuk, R. Lodge, T. Roberts, K. Hirschberg, R. Phair, and J. Lippincott-Schwartz. 2001. Rapid cycling of lipid raft markers between the cell surface and Golgi complex. *J. Cell Biol.* **153:** 529–541.

49. Khine, A. A., P. Tam, A. Nutikka, and C. A. Lingwood. 2004. Brefeldin A and filipin distinguish two globotriaosyl ceramide/verotoxin-1 intracellular trafficking pathways involved in Vero cell cytotoxicity. *Glycobiology.* **14:** 701–712.

50. Sandvig, K., E. Dubiniana, O. Garred, K. Prydz, J. V. Kozlov, S. H. Hansen, and B. van Deurs. 1992. Protein toxins: mode of action and cell entry. *Biochem. Soc. Trans.* **20:** 724–727.

51. Johannes, L., D. Tenza, C. Anthony, and B. Goud. 1997. Retrograde transport of KDEL-bearing B-fragment of Shiga toxin. *J. Biol. Chem.* **272:** 19554–19561.

52. Saint-Pol, A., B. Yelamos, M. Amessou, I. G. Mills, M. Dugast, D. Tenza, P. Schu, C. Antony, H. T. McMahon, C. Lamaze, et al. 2004. Clathrin adaptor epsinR is required for retrograde sorting on early endosomal membranes. *Dev. Cell.* **6:** 525–538.

53. Arab, S., M. Murakami, P. Dirks, B. Boyd, S. Hubbard, C. Lingwood, and J. Rutka. 1998. Verotoxins inhibit the growth of and induce apoptosis in human astrocytoma cells. *J. Neurooncol.* **40:** 137–150.

54. Hoey, D. E. E., C. Currie, C. A. Lingwood, D. L. Gally, and D. G. E. Smith. 2003. Binding of verotoxin 1 to primary intestinal epithelial cells expressing Gb3 results in trafficking of toxin to lysosomal compartments. *Cell. Microbiol.* **5:** 85–97.

55. Falg[u]ieres, T., W. Romer, M. Amessou, C. Afonso, C. Wolf, J. C. Tabet, C. Lamaze, and L. Johannes. 2006. Functionally different pools of Shiga toxin receptor, globotriaosyl ceramide, in HeLa cells. *FEBS J.* **273:** 5205–5218.

56. Puri, A., P. Hug, K. Jernigan, J. Barchi, H-Y. Kim, J. Hamilton, J. Wiels, G. J. Murray, R. O. Brady, and R. Blumenthal. 1998. The neutral glycosphingolipid globotriaosylceramide promotes fusion mediated by a CD4-dependent CXCR4-utilizing HIV type 1 envelope glycoprotein. *Proc. Natl. Acad. Sci. USA.* **95:** 14435–14440.

57. Fantini, J., D. Hammache, O. Delezay, N. Yahi, C. Andre-Barres, I. Rico-Lattes, and A. Lattes. 1997. Synthetic soluble analogs of galactosylceramide (GalCer) bind to the V3 domain of HIV-1 gp

lipid-containing lipid mixtures as raft models of plasma membrane. *J. Phys. Condens. Matter.* **17:** S2965–S2977.

120 and inhibit HIV-1-induced fusion and entry. *J. Biol. Chem.* **272:** 7245–7252.

58. Martensson, E. 1966. Neutral glycolipids of human kidney isolation, identification, and fatty acid composition. *Biochim. Biophys. Acta.* **116:** 296–308.

59. Mizutani, Y., A. Kihara, and Y. Igarashi. 2005. Mammalian Lass6 and its related family members regulate synthesis of specific ceramides. *Biochem. J.* **390:** 263–271.

60. Pewzner-Jung, Y., S. Ben-Dor, and A. H. Futerman. 2006. When do Lasses (longevity assurance genes) become CerS (ceramide synthases)? Insights into the regulation of ceramide synthesis. *J. Biol. Chem.* **281:** 25001–25005.

61. Wisniewska, A., J. Draus, and W. K. Subczynski. 2003. Is a fluid-mosaic model of biological membranes fully relevant? Studies on lipid organization in model and biological membranes. *Cell. Mol. Biol. Lett.* **8:** 147–159.

62. Ångström, J., S. Tennenberg, M. Abul-Milh, I. Leonardsson, M. Ölwegård-Halvarsson, Å. Ljung, T. Wadström, and K-A. Karlsson. 1998. The lactosylceramide binding specificity of *Helicobacter pylori.* *Glycobiology.* **8:** 297–309.

63. de Almeida, R., A. Fedorov, and M. Prieto. 2003. Sphingomyelin/phosphatidylcholine/cholesterol phase diagram: boundaries and composition of lipid rafts. *Biophys. J.* **85:** 2406–2416.

64. Groves, J. T. 2007. Bending mechanics and molecular organization in biological membranes. *Annu. Rev. Phys. Chem.* **58:** 697–717.

65. Brown, D., and E. London. 1998. Functions of lipid rafts in biological membranes. *Annu. Rev. Cell Dev. Biol.* **14:** 111–136.